Article

A Reversible and Distance-Controllable DNA Scissor: A Regenerated Electrochemiluminescence Biosensing Platform for Ultrasensitive Detection of MicroRNA

Lichun Peng, Yali Yuan, Xiaomin Fu, Ao Fu, Pu Zhang, Yaqin Chai, Xianxue Gan, and Ruo Yuan

Anal. Chem., **Just Accepted Manuscript** • DOI: 10.1021/acs.analchem.8b02757 • Publication Date (Web): 01 Feb 2019

A Reversible and Distance-Controllable DNA Scissor: A Regenerated Electrochemiluminescence Biosensing Platform for Ultrasensitive Detection of MicroRNA

Lichun Peng[1a], Yali Yuan[1a], Xiaomin Fu[b], Ao Fu[a], Pu Zhang[a], Yaqin Chai[a], Xianxue Gan*[b], Ruo Yuan*[a]

[a]Key Laboratory of Luminescent and Real-Time Analytical Chemistry（Southwest University）, Ministry of Education, School of Chemistry and Chemical Engineering, Southwest University, Chongqing 400715, PR China

[b]College of Chemistry and Chemical Engineering, Yibin University, Yibin, Sichuan 644007, PR China

* Corresponding author. Tel.: +86-23-68252277; Fax: +86-23-68253172.

E-mail address: ganxianxue@sina. com, yuanruo@swu.edu.cn;

[1]The first two authors have equal contribution to the work.

ABSTRACT

Reversing the switching of DNA scissors with precisely control remains a compelling goal. Herein, based on strand displacement reaction within single step, the DNA scissor realized reversible switching and further controlled the distance of end strands along the movement of DNA scissor, which has been applied for the development of a regenerated sensing platform for the ultrasensitive detection of microRNA-21 (miRNA-21) with the electrochemiluminescence (ECL) complex (PEI-Ru(II)) as luminophores and diethylenetriamine (DETA) as the coreactant. In the presence of ferrocene-labeled DNA (Fc-DNA), the DETA-labeled DNA scissor clockwise switched to "off" state based on strand displacement reaction, resulting in the significant ECL quenching of Ru(II) system. Next, by using miRNA-21 as the motive fuel, the configuration of DNA scissor could be anticlockwise switched, which significantly enhanced the ECL intensity of Ru(II) complex due to the releasing of Fc-DNA and the proximity between DETA and Ru(II) complex. The reversible switching of DNA scissor led to the remarkably enhancing of ECL signal, realizing ultrasensitive detection of miRNA-21 with an excellent detection limit of 0.17 fM, which was also applied in miRNA detection successfully from different cancer cells. Impressively, the reversible switching of DNA scissor biosensor was able to realize the regeneration of the biosensing platform by adding an additional single stranded DNA (ssDNA) based on strand displacement reaction within single step, providing a novel concept for constructing simple and sensitive regenerated biosensor.

KEYWORDS: DNA scissor, biosensor, electrochemiluminescent, microRNA.

INTRODUCTION

Being the most exciting biomolecule, DNA has the promising potential for wide employment in nanotechnology and material science.[1-4] Due to its excellent functions which originated from structure, composition, as well as chemical and physical properties, DNA as the central fundamental material is available to synthesize artificial nanostructrues.[5] Significantly, with the involvement of a specific number of DNA double helices, these nanostructures can perform special mechanical functionality and imitate biological phenomena.[6] On the basic of the desirable performance, the diversity of nanostructures, especially DNA-based nanodevices and nanomachines, have gained substantial research interests.[7,8] Therefore, the DNA-based devices such as "walkers",[9] "tweezers",[10] "motors",[11] "gears",[12] and other nanodevices[13-15] have been developed to mimic the machinery functionalities, which represent an impressive research topic in DNA nanostructures. For example, Seeman's group has recently reported a DNA origami scissor device which was designed by incorporating two double-crossovers (DX) molecules into a flexible Holliday junction, and the scissor was actuated into an opened state upon binding of MutS.[16] Although the reported DNA origami scissor could perform larger-scale structural conformational changes, the conformational switching of the DNA scissor is disposable because the sticky ends was disrupted by DNA-bending proteins. Therefore, exploring a reversible switching of DNA scissor with precisely control which could realize regeneration is a significant issue for broadening the application of DNA nanodevices.

As the regulators of gene expression, microRNAs (miRNAs) can decrease the stability or repress translation of the target miRNAs.[17] Previous studies have demonstrated that miRNAs can play a role of a significant biomarker for the diacrisis of various genetic disorders and cancers.[18] Although various progressive techniques have been applied to miRNA analyses, it is still a great

challenge to regenerate the biosensing, which can provide a reagentless and cost-effective detection system. Recently, based on Exonuclease III-catalyzed regeneration of the biomarker, a multiplexed detection system was fabricated by Willner'group by using functionalized quantum dots (QDs).[19] Furthermore, our group has reported a biosensor that realized the regeneration by multi-step strand displacement reactions for multiple electrochemiluminescence(ECL) detections of miRNAs based on DNA nanogears.[20] Although, the reported studies realized the regeneration of sensing, these studies were short of easy operation, low cost, time and labor consumption, primarily limited the applicable scope of the biosensor.[21] Herein, a miRNA fueled-DNA scissor with distance controllability can achieve the regeneration of sensing platform within one-step reaction, which represent an advance over the previous DNA scissors and is of great significance on DNA nanodevice development in the progress of sensing platform.

The designed reversible switching of the DNA scissor could perform continuous anticlockwise and clockwise switching with the control of nucleic acid to control the distance of end strands and achieve the regeneration within one-step reaction. Inspired by the reversible switching of DNA scissor, we designed a regenerated ECL biosensor for the highly sensitive analysis of biomarkers. As exhibited in Scheme 1, firstly, the luminous Ru(II) complex which contained PEI [poly(ethylenimine)] and $Ru(dcbpy)_3Cl_2$ [Tris(4,4'-dicarboxylicacid-2,2'-bipyridyl)ruthenium(II) dichloride] as ECL emitter were modified on the sensing surface by using the film-forming property of PTCA (3,4,9,10-perylene tetracarboxylic acid) *via* amide bond. At the same time, the designed DNA scissor was composed with different DNA strands (S1-S10) which contained coreactant of DETA-labeled S1 and DETA-labeled S3 strands with three exposures of A, B, C. Secondly, the DNA scissor was incubated on the PTCA-PEI-Ru(II) film-modified electrode. Subsequently,

ferrocene-labeled DNA (Fc-DNA) was introduced to hybridize with the end strands of A/B, realizing the anticlockwise switching of the DNA scissor to achieve the "off" state and quenching the initial ECL intensity of the Ru(II) complex due to radical reactions and electron transfer between ferrocene and the Ru(II) complex.[22] Simultaneously, the DETA-labeled end strand (DETA-A) and sensing surface were at a large separation. When the target miRNA-21 was introduced to displace Fc-DNA based on toehold-mediated strand displacement reactions (TSDR) and hybridize with the end strands of B/C, the DNA scissor clockwise switched to "on" state and DETA-A was close to PTCA-PEI-Ru(II) film. Significantly, the ECL signal was enhanced considerably because Fc-DNA was replaced by miRNA-21 and the closure between DETA-A and PTCA-PEI-Ru(II) film which shortened electronic transmission distance and improved luminous efficiency. Impressively, after the incubation of an additional single stranded DNA (ssDNA) which was fully hybridized with miRNA-21 to produce duplex waste, the DNA scissor switched into the "open" state and the biosensor was regenerated due to strand displacement reaction within single step. On the basic of the reversible switching of the DNA scissor, the ECL biosensor for miRNA detection exhibited a wide linear range from 0.5 fM to 10 pM and a detection limit of 0.17 fM, being applied to MCF-7 (human breast cancer cells) analysis. Incorporating with the original technology, the DNA machine has bright perspective for further research in the potential applications of biomedical research and clinical diagnostics.

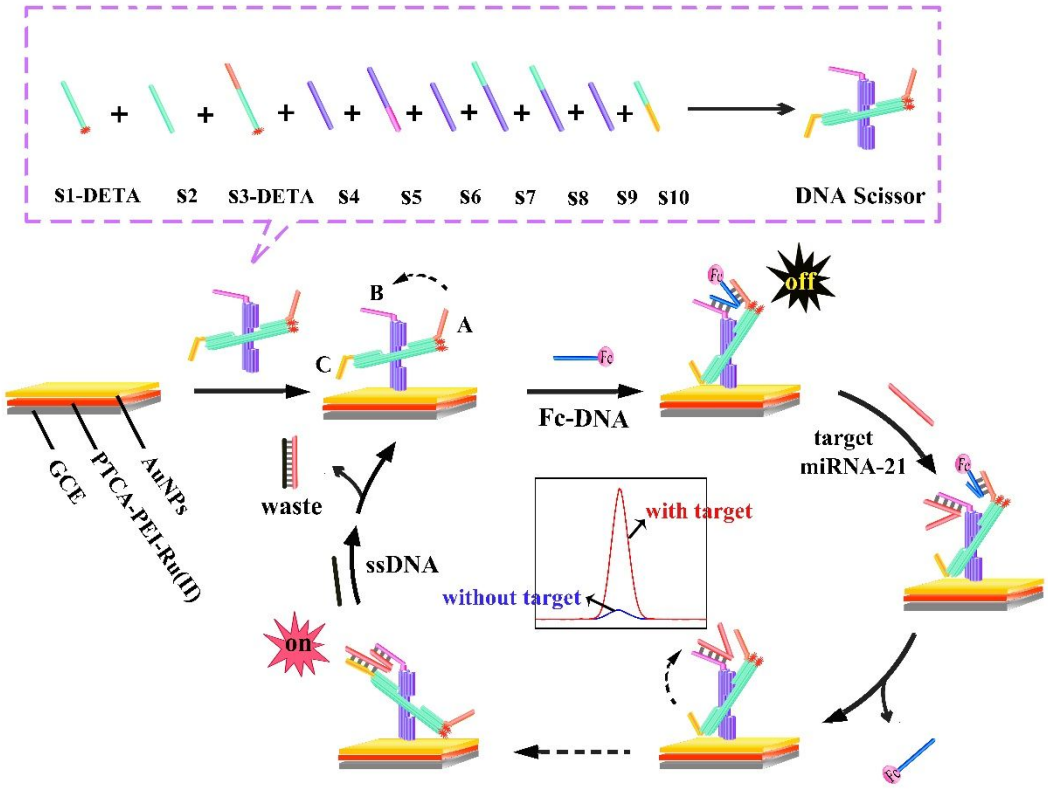

Scheme 1. Working principle of the reversible and distance-controllable DNA scissor-based regenerated biosensor for miRNA-21 detection.

EXPERIMENTAL SECTION

Preparation of Ru(II) Complex. The Ru(II) complex (PTCA-PEI-Ru(II)) was synthesized according to our previous method with slight modifications.[23] First, 2 mL of solution (10 mM of NHS and40 mM of EDC) was dispersed with 0.5 mL of 25.0 mM $Ru(dcbpy)_3Cl_2$ solution. The mixed solution was incubated in ice water bath with 4 h under constant stirring. Next, the solution of PEI (0.6 M) was mixed with the previous solution. After stirring the solution at 4 °C for 12 h, the PEI-Ru(II) compound was prepared *via* the formation of amide bonds.

Meanwhile, the PTCA solution was synthesized according the method reported in our previous.[23] Briefly, the above PEI-Ru(II) compound was stirring at 4 °C for 12 h, which was

cross-linked with the prepared PTCA *via* amide bond. Afterward, the final compound was centrifuged for 15 min and resuspended in 0.1 M PBS (pH 7.0). The proposed Ru(II) complex was characterized by SEM in Figure S2B.

According to a reported protocol,[24] AuNPs were synthesized by citrate reduction of $HAuCl_4$. The average particle size was characterized by SEM (Figure S2C) and appeared an average diameter of 16±1 nm.

Preparation of DNA Scissors. The S1-DETA, S3-DETA as co-reactant were developed *via* the formation of amide bond between the carboxyl groups of the DNA strands (S1, S3) and the amino group of DETA. First, the carboxyl modified DNA strands (S1 and S3, 24 μM) were respectively mixed with 40 mM of EDC and 10 mM of NHS in HEPES buffer. After being added with DETA (1.8 mM) into the activated DNA for 3 h, the resulted solution was stored at -20 °C.

In the process, S1-DETA and S3-DETA were employed with the mixture of DNA strands (S2 and S4-S10, 24 μM) in HEPES buffer. The above mixture was heated to 90 °C. Then, the obtained solution was cooled slowly to 37 °C during 40 h for the formation of the DNA scissor. At last, the complex was removed into a dialysis tube with centrifugal filter devices (MWCO 8000).

Construction of the Designed miRNA Sensor. The polished GCE was first modified with 20 μL of the obtained Ru(II) complex. Then, the complex was dried in air to acquire a Ru(II) complex film. Subsequently, the obtained electrode was soaked in AuNPs solution for 8 h by the interaction of Au-S covalent bond. After that, 20 μL of the DNA scissor was assembled on the surface of the AuNPs/PTCA-PEI-Ru(II) film *via* Au-S covalent bond and incubated overnight at room temperature. Eventually, the proposed biosensor was further modified with Fc-DNA and miRNA-21 for 1h successively. To achieve the regeneration of the biosensor, the assembled biosensor was incubated

with an additional single stranded DNA (ssDNA) for 1h.

Native Polyacrylamide Gel Electrophoresis (PAGE). The different obtained samples were subjected to electrophoresis analysis on the notches of the 10% PAGE. Electrophoresis was performed in 1× TBE at 80 V for 160 min, and then the gels were stained with ethidium bromide (EB). Above all, the electrophoresis imaging was taken by a Bio-Rad Gel Doc XR + System.

RESULTS AND DISCUSSION

Investigation of the DNA Scissor. The designed DNA scissor was characterized by PAGE. As Figure 1 described, incubation of S1-S10 strands led to the formation of DNA scissor with a distinct single band (lane 1), indicting the scissor were stable nanostructures. After the introduction of Fc-DNA, comparing with lane 1, a higher band (lane 2) was obtained because the complex had a larger molecular weight, indicating the successful hybridization of Fc-DNA and DNA scissor. As expected, miRNA-21 could hybridize with DNA scissor and displace Fc-DNA which was driven thermodynamically by entropy, which was verified by the distinct band (lane 3) with slight lower mobility. Furthermore, when ssDNA fully hybridized with miRNA-21, the proposed band (lane 4) exhibited a fast mobility with lower molecular weight, demonstrating the regeneration of DNA scissor. These PAGE results demonstrated that the process of the DNA scissor was successful and feasible.

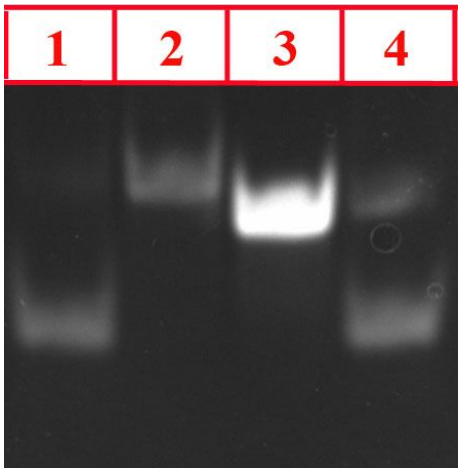

Figure 1. PAGE characterization of the obtained samples. Lane 1: DNA scissor; Lane 2: Fc-DNA + DNA scissor; Lane 3: miRNA-21 + Fc-DNA + DNA scissor; Lane 4: ssDNA + miRNA-21 + DNA scissor.

Electrochemical Characterization of the Designed Biosensor. In order to monitor the stepwise modified electrochemical biosensor, CVs were employed to measure different assembled electrodes. As can be seen from Figure 2, a pair of the apparent redox peak of $[Fe(CN)_6]^{3-/4-}$ (curve a) was exhibited on bare GCE. A subsequent incubation of PTCA-PEI-Ru(II) on the sensing surface caused an obvious increment of the current due to the electroconductive properties of PTCA-PEI-Ru(II) (curve b). When absorbed with AuNPs, the CV curve (curve c) increased apparently because of the excellent conductivity of AuNPs for promoting the electron transfer. After the incubation of DNA scissor, the redox current decreased evidently (curve d), suggesting that DNA chains had nonelectroactive character to hinder the electron transfer. Then, the current declined successively under the introduction of Fc-DNA (curve e), indicating that Fc-DNA inhibited the transmission of electrons. It was observed that the CV curve (curve f) was increased because Fc-DNA had a larger molecule comparing with miRNA-21. At last, the incubation of ssDNA led to a slight restoration of the CV curve (curve g vs. d), because ssDNA fully hybridized with miRNA-21

to regenerate the biosensor.

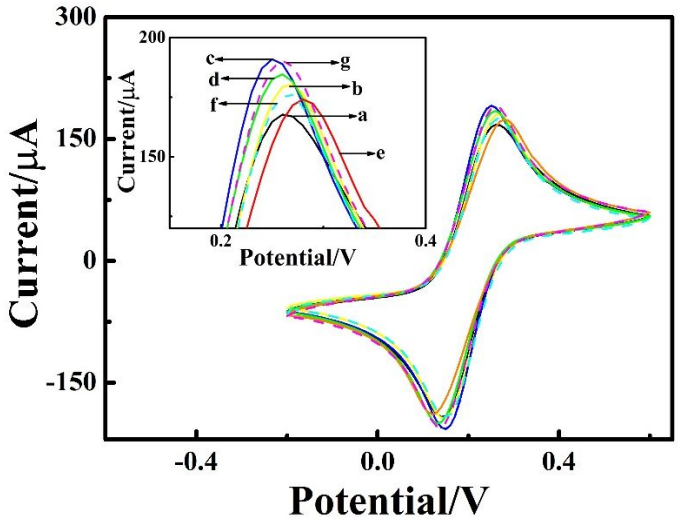

Figure 2. CV profiles of the stepwise modified electrodes: (a) bare GCE, (b) modified with Ru(II) complex, (c) employed with AuNPs, (d) decorated with DNA scissor, (e) employed with Fc-DNA, (f) introduced with miRNA-21, and (f) regenerated by ssDNA. The CVs were measured in 5.0 mM $[Fe(CN)_6]^{3-/4-}$ at a scan rate of 100 mV/s with scanning the potential from -0.2 to 0.6 V. Inset: magnified CV curves.

ECL Performance of the Designed Biosensor. The ECL signals were monitored to evaluate different assembled electrodes in PBS (pH=7.0). As can be seen from Figure 3, on a bare GCE, no ECL response was achieved because of the absence of ECL luminophore (curve a). When PTCA-PEI-Ru(II) compound was modified on the GCE, owing to the introduction of luminescence reagent, a remarkable ECL response was acquired (curve b). Upon modification of AuNPs *via* Au-NH, an increased ECL intensity was obtained, testing the electron transfer was facilitated by AuNPs. After the incubation of DNA scissor, the ECL intensity increased successively because of the introduction of DETA as coreactant toward Ru(II) ECL system (curve d). Subsequently, when the resultant biosensor was incubated with Fc-DNA, a desirable "off" state was obtained owing to

the quench property of Fc-DNA toward Ru(II) complex (curve e). However, the biosensor switched to "on" state after introducing miRNA-21 (curve f) to displace Fc-DNA, demonstrating that the proximity of Ru(II) complex film and DETA could improve the ECL efficiency of Ru(II). Finally, ssDNA incubated on the electrode in order to the regeneration of the biosensor (curve g). Impressively, the regeneration of the biosensor led to a decreasing of the ECL curve (curve g vs. f) because the intermolecular distance between DETA and PTCA-PEI-Ru(II) film became larger, primitively demonstrating the distance-controllable luminous efficiency between Ru(II) complex and coreactant.

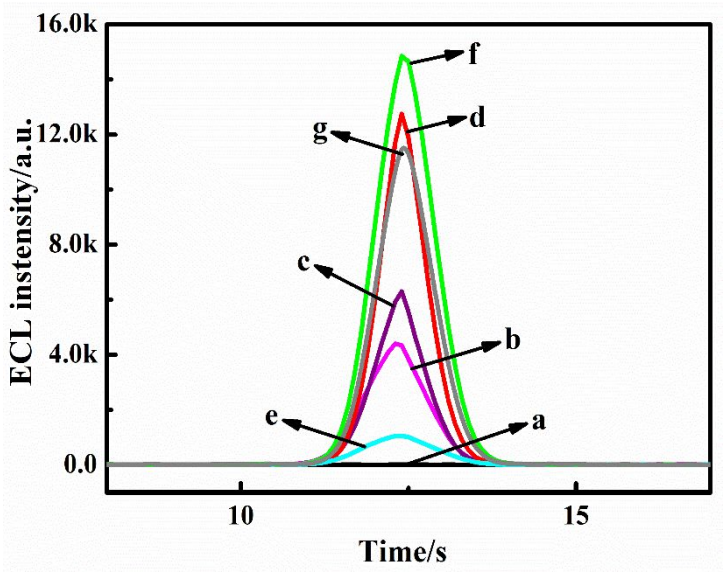

Figure 3. ECL-time curves of different electrodes: (a) bare GCE, (b) modified with Ru(II) complex, (c) employed with AuNPs, (d) decorated with DETA-labled DNA scissor, (e) employed with Fc-DNA, (f) introduced with miRNA-21, and (g) regenerated by ssDNA with a scan rate of 100 mV/s by setting the potential between 0 and 1.25 V.

Optimization of the Detected Condition. To obtained optimal performance of the constructed biosensor by using our system, experimental parameters containing the volume of Ru(II) complex and the concentration of DETA were investigated. The ECL intensity (Figure 4A) increased

gradually with the volume of Ru(II) complex up to 20 μL and reached a relative stable value when the volume was greater than 20 μL. As a result, 20 μL was chosen as the optimal volume of PTCA-PEI-Ru(II) in this work. Furthermore, the concentration of DETA was also an important parameter to influence the performance of biosensor. In Figure 4B, with the increase of the concentration of DETA, the ECL signal enhanced rapidly and then reached a constant value at 1.8 mM. Thus, the concentration of DETA of 1.8 mM was the optimal choice in the proposed biosensor.

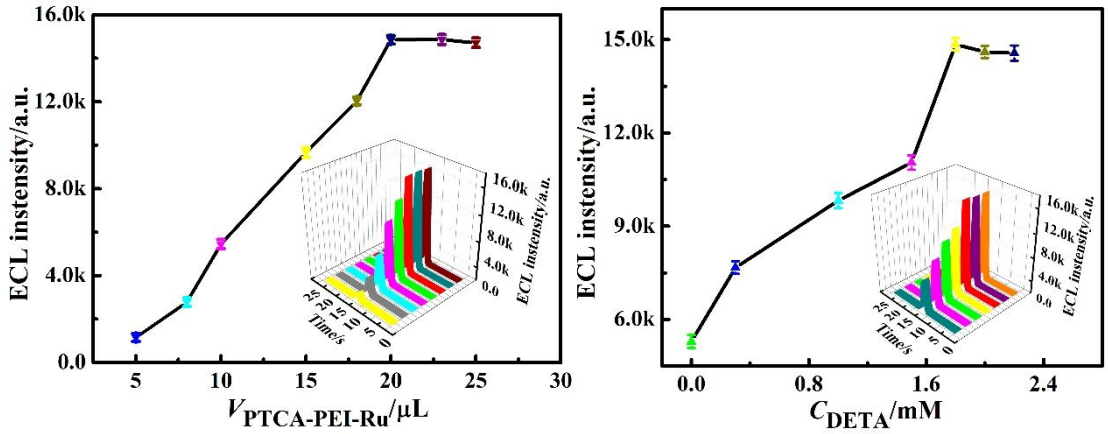

Figure 4. The optimization of (A) the volume of Ru(II) complex and (B) the concentration of DETA which was modified with S1 and S3 strand. The ECL intensity of the obtained biosensor was measured in 2.5 mL of PBS (pH 7.0). Error bars: standard deviation (SD), n = 3.

Detection of miRNA-21 with the Constructed Biosensor. Under optimized laboratorial conditions, the excellent dependence of the ECL responses of the elaborate biosensor were used to detect miRNA-21 with different concentrations. According to Figure 5, the ECL response (curves a-f) prominent increased with increasing concentration of miRNA-21 in the range from 0.5 fM to 10 pM. The linear equation was $y = 11545.6 + 2975.5 \log c$ (where y represented the ECL intensity and c represented the concentration of target), and the measured detection limit was 0.17 fM. The estimated square correlation coefficient was 0.9957. Furthermore, from Table 1, the comparison for

previous reports of miRNA detection illustrated that this designed system would hold a wider application for sensitive bioassays in clinical detection. The reason can be ascribed to the following two reasons: first, the immobilization of large amounts of luminescence reagent PTCA-PEI-Ru(II) containing luminophore and coreactant in the same complex on electrode surface, can effectively enhance the ECL intensity with improved sensitivity of proposed approach. Second, the PTCA assembled on electrode can provide a large surface area for loading abundant luminophore and coreactant, which also improved the sensitivity.

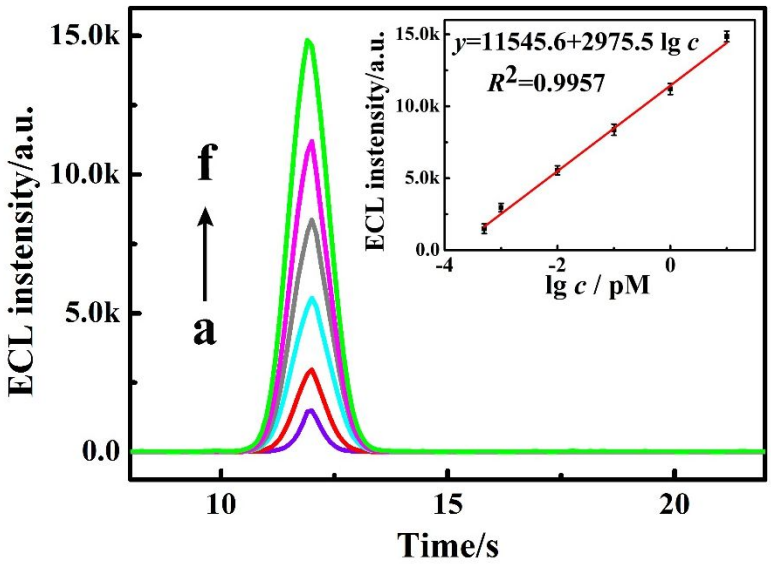

Figure 5. ECL-time curves of DNA scissor biosensor in the presence of different concentrations of the target miRNA-21. (a) 0.5 fM, (b) 1 fM, (c) 0.01 pM, (d) 0.1 pM, (e) 1 pM, (f) 10 pM. Scan rate, 100 mV/s.

Table 1. Comparison of our research with other methods for miRNA detection.

Analytical methods	Linear range	Detection limit	Ref.
fluorescent	10 pM~100 pM	8.4 pM	25
fluorescent	3.8 pM~10 nM	3.8 pM	26
surface enhanced Raman scattering	10 fM~100 pM	10 fM	27
surface enhanced Raman scattering	0.5 nM~5 nM	485 pM	28
Electrochemical	500 fM~5 nM	100 fM	29
ECL	10 fM~10 pM	10 fM	30
ECL	1 fM~100 pM	1 fM	31
ECL	0.5 fM~10 pM	0.17 fM	*This work*

Related Performance of the ECL Biosensor. The reproducibility, stability, and selectivity are importance to confirm the performances of the biosensor. As seen from Figure S3**,** the calculated relative standard deviations (RSDs) were 3.87% and 4.01%. These results demonstrated that the constructed biosensor presented an excellent reproducibility.

On the other hand, as shown in Figure 6A, the ECL stability was evaluated adequately under a three cycles' potential scan to various concentrations of miRNA-21. With the increasing of miRNA-21 concentration, the ECL response increased gradually, and on obvious changes could be observed at every concentration. The experimental result indicated that the stability of the using system was superior.

According to Figure 6B, the selectivity of the biosensors was evaluated by interfering agents, including miRNA-155 (100 pM), miRNA-199a (100 pM), miRNA-141 (100 pM) and one-base

mismatched miRNA-21 (100 pM). As expected, the interfering agents caused minimal ECL signal. However, when analyzed respectively 10 pM of miRNA-21and the mixtures containing 100 pM of every interfering agents and 10 pM of miRNA-21, the ECL intensity exhibited conspicuous signals compared to the interfering agents. The results demonstrated the favorable selectivity of the designed biosensor.

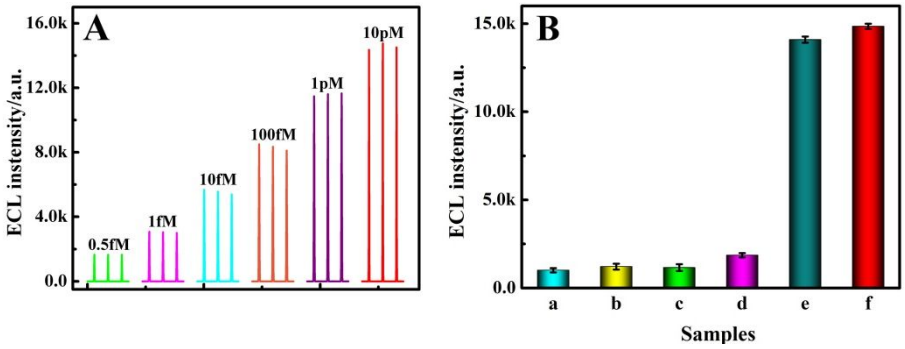

Figure 6. (A) Stability of the proposed biosensor to various concentrations of miRNA-21. (B) Selectivity of the obtained biosensor when analyzed with (a) 100 pM of miRNA-155, (b) 100 pM of miRNA-199a, (c)100 pM of miRNA-141, (d)100 pM of one-base mismatched miRNA-21 (e) 10 pM of miRNA-21 in mixed solution, and (f) 10 pM of miRNA-21.

Regenerability. To judge the regenerability of the constructed biosensor, ssDNA was introduced to completely hybridized to miRNA-21 and realized regeneration of the biosensor. As presented in Figure 7A, comparing to the original "on" state (curve a), the ECL response (curve b) was significantly increased when detected the target. Notably, after the addition of ssDNA, the proposed biosensor regenerated with an excited ECL intensity of 98.3% (curve c). In addition, the biosensor could be regenerated and was stable enough to analysis miRNA-21 over 4 cycles (Figure 7B). The result indicates that the constructed biosensor has an ideal regenerability, and therefore it can be seen that the sensing platform based on the nanomachine has another outstanding advantage. The result obtained in this work demonstrates that the DNA scissor-based biosensor endows

excellent regenerability, which holds great advantages for expanding the application of clinical diagnose.

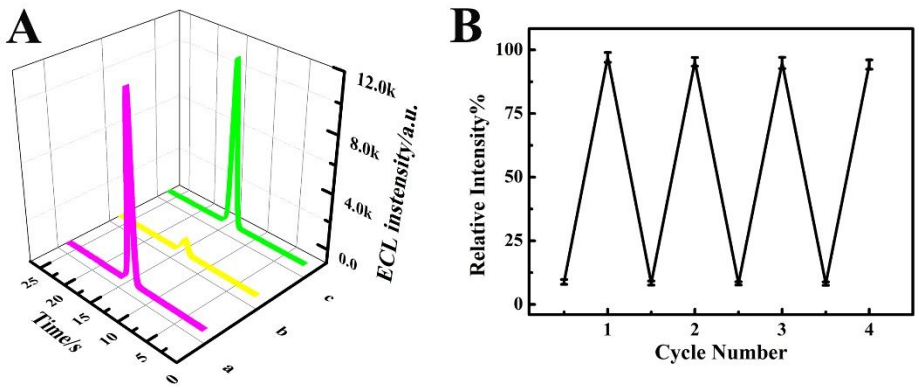

Figure 7. (A) ECL response of the regenerated biosensor: the "on" state of the biosensor (curve a), "off" state of the biosensor (curve b), and regeneration of the biosensor with the representation of the "on" state (curve c). (B) ECL intensity for target detection over four cycles.

Application. To explore the application of the developed biosensor, MCF-7 (human breast cancer) cells and HeLa (human cervical cancer) cells were selected to confirm the expression of miRNA-21. After cell counting, the cell samples were extracted by using the Trizol Reagent Kit to extract the total RNA samples. Furthermore, the cell concentrations of the two cancer cells from 100 cells to 10^5 cells were used to measure the sensitivity of the designed biosensor. As the results depicted in Figure 8, the ECL intensity of the designed biosensor with HeLa cells caused slight increases to the cell concentrations increase from 100 cells to 10^5 cells. However, the obtained biosensor with the extraction of MCF-7 cells had significant ECL intensity with the cell concentrations increased from 100 cells to 10^5 cells. The above results which were consistent with existing reports manifested the high expression of miRNA-21 in MCF-7 cells rather than HeLa cells.[32, 33]

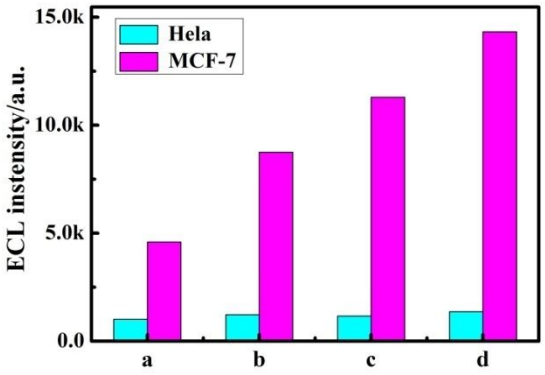

Figure 8. Analysis of miRNA-21 from MCF-7 and HeLa cells: (a) 100 cells; (b) 10^3 cells; (c) 10^4 cells; (d) 10^5 cells.

CONCLUSION

In this article, we proposed a reversible and distance-controllable DNA scissor activated by miRNA and applied it in an ECL enzyme-free biosensor for sensitive detection of the miRNA cancer biomarker. The elaborated biosensor presented two innovative ideas. First, with the activation of miRNA, the DNA scissor could perform successive transformation which realized the reversible switching and further controlled the distance between DETA and PTCA-PEI-Ru(II) film for the improvement of ECL response, thus expanding the promising application of DNA nanomachines in biosensing. Second, the distance-controllability of DNA scissor enabled the proposed ECL biosensor to be regenerated through strand displacement reaction, which had the advantage of time and labor-saving compared to the traditional sensing platform. Moreover, with the ingenious construction of DNA scissor, the well-designed biosensor laid a bright prospect in biosensing and various biomarkers analysis.

ASSOCIATED CONTENT

Supporting Information

Additional electronic information as pointed in the essay. This information is available free of charge via the Internet at http://pubs.acs.org

Reagents and materials, the oligonucleotides sequences used in this work, characterization of the proposed materials, reproducibility of the proposed biosensor.

ACKNOWLEDGEMENTS

This work was financially supported by the NNSF of China (21775124, 21675129, 21505107, 21575116 and 51473136), Fundamental Research Funds for the Central Universities (XDJK2018AA003).

REFERENCES

(1) Aldaye, F. A.; Palmer, A. L.; Sleiman, H. F. Assembling Materials with DNA as the Guide. *Science* **2008**, *321*, 1795-1799.

(2) Dave, N.; Liu, J. W. Programmable Assembly of DNA-Functionalized Liposomes by DNA. *ACS Nano* **2011**, *5* 1304-1312.

(3) Hansen, M. H.; Blakskjær, P.; Petersen, L. K.; Hansen, T. H.; Højfeldt, J. West.; Gothelf, K. V.; Hansen, N. J. V. A Yoctoliter-Scale DNA Reactor for Small-Molecule Evolution. *J. Am. Chem. Soc.* **2009**, *131*, 1322-1327.

(4) Wu, L.; Ding, F.; Yin, W. N.; Ma, J.; Wang, B. R.; Nie, A. X.; Ding, F.; Han, H. Y. From Electrochemistry to Electroluminescence: Development and Application in a Ratiometric Aptasensor for Aflatoxin B1. *Anal. Chem.* **2017**, *89*, 7578-7585.

(5) Kuzyk, A.; Schreiber, R.; Fan, Z. Y.; Pardatscher, G.; Roller, E. M.; Högele, A.; Simmel, F. C.; Govorov, A. O.; Liedl, T. DNA-Based Self-assembly of Chiral Plasmonic Nanostructures with Tailored Optical Response. *Nature* **2012**, *483*, 311-314.

(6) Stewart, K. M.; Mclaughlin, L. W. Four-Arm Oligonucleotide Ni(II)-Cyclam-Centered Complexes as Precursors for the Generation of Supramolecular Periodic Assemblies. *J. Am. Chem. Soc.* **2004**, *126*, 2050-2057.

(7) Beissenhirtz, M. K.; Willner, I. DNA-Based Machines. *Org. Biomol. Chem.* **2006**, *4*, 3392-3401.

(8) Ma, J.; Wu, L.; Li, Z. H.; Lu, Z. C.; Yin, W. M.; Nie, A. X.; Ding, F.; Wang, B. R.; Han, H. Y. Versatile Electrochemiluminescence Assays for PEDV Antibody Based on Rolling Circle Amplification and Ru-DNA Nanotags. *Anal. Chem.* **2018**, *90*, 7415-7421.

(9) Wang, Z. G.; Elbaz, J.; Willner, I. DNA Machines: Bipedal Walker and Stepper. *Nano Lett.* **2011**, *11*, 304-309.

(10) Zhou, C.; Yang, Z. Q.; Liu, D. S. Reversible Regulation of Protein Binding Affinity by a DNA Machine. *J. Am. Chem.Soc.* **2012**, *134*, 1416-1418.

(11) Pavlick, R.; Dey, K.; Sirjoosingh, A.; Benesia, A.; Sen, A. A Catalytically Driven Organometallic Molecular Motor. *Nanoscale* **2013**, *5*, 1301-1304.

(12) Tian, Y.; Mao, C. Molecular Gears: A Pair of DNA Circles Continuously Rolls Against Each Other. *J. Am. Chem. Soc.* **2004**, *126*, 11410-11411.

(13) Kuzuya, A.; Sakai, Y.; Yamazaki, T.; Xu, Y.; Komiyama, M. Nanomechanical DNA Origami Single-Molecule Beacons Directly Imaged by Atomic Force Microscopy. *Nat. Commun.* **2011**, *2*, 449-457.

(14) Mao, C. D.; Sun, W. Q.; Shen, Z. Y.; Seeman, N. C. A Nanomechanical Device Based on the B-Z Transition of DNA. *Nature* **1999**, *397*, 144-146.

(15) Zhang, Q.; Chen, F.; Xu, F.; Zhao, Y. X.; Fan, C. H. Target-Triggered Three-Way Junction

Structure and Polymerase/Nicking Enzyme Synergetic Isothermal Quadratic DNA Machine for Highly Specific, One-Step, and Rapid MicroRNA Detection at Attomolar Level. *Anal. Chem.* **2014**, *86*, 8098-8105.

(16) Gu, H. Z.; Yang, W.; Seeman, N. C. DNA Scissors Device Used to Measure MutS Binding to DNA Mis-pairs. *J. Am. Chem. Soc.* **2010**, *132*, 4352-4357.

(17) Fabian, M. R.; Sonenberg, N.; Filipowicz, W. Regulation of MRNA Translation and Stability by MicroRNAs. *Annu. Rev. Biochem.*, **2010**, *79*, 351-379.

(18) Kosaka, N.; Iguchi, H.; Ochiya, T. Circulating MicroRNA in Body Fluid: a New Potential Biomarker for Cancer Diagnosis and Prognosis. *Cancer Sci.* **2010**, *101*, 2087-2092.

(19) Freeman, R.; Liu, X. Q.; Willner, I. Amplified Multiplexed Analysis of DNA by the Exonuclease III-Catalyzed Regeneration of the Target DNA in the Presence of Functionalized Semiconductor Quantum Dots. *Nano Lett.* **2011**, *11*, 4456-4461.

(20) Zhang, P.; Lin, Z. F.; Zhuo, Y.; Yuan, R.; Chai, Y. Q. Dual microRNAs-Fueled DNA Nanogears: A Case of Regenerated Strategy for Multiple Electrochemiluminescence Detection of microRNAs with Single Luminophore. *Anal. Chem.* **2017**, *89*, 1338-1345.

(21) Zhang, X. B.; Liu, C. H.; Sun, L. B.; Duan, X. R.; Li, Z. P. Lab on a Single Microbead: an Ultrasensitive Detection Strategy Enabling microRNA Analysis at the Single-molecule Level. *Chem. Sci.* **2015**, *6*, 6213-6218.

(22) Cao, W. D.; Ferrance, J. P.; Demas, J.; Landers, J. P. Quenching of the Electrochemiluminescence of Tris(2,2‘-bipyridine)ruthenium(II) by Ferrocene and Its Potential Application to Quantitative DNA Detection. *J. Am. Chem. Soc.* **2006**, *128*, 7572-7578.

(23) Zhao, Min.; Liao, N.; Zhuo, Y.; Chai, Y. Q.; Wang, J. P.; Yuan, R. Triple Quenching of a Novel

Self-Enhanced Ru(II) Complex by Hemin/G-Quadruplex DNAzymes and Its Potential Application to Quantitative Protein Detection. *Anal. Chem.* **2015**, *87*, 7602-7609.

(24) Crabar, K. C.; Freeman, R. G.; Hommer, M. B.; Natan, M. J. Preparation and characterization of Au colloid monolayers. A*nal. Chem*. **1995**, *67*, 735-743.

(25) Niu, C. X.; Song, Q. w.; He, G.; Na, N.; Ouyang, J. Near-infrared-fluorescent Probes for Bioapplications Based on Silica-coated Gold Nanobipyramids with Distance-dependent Plasmon-enhanced Fluorescence. *Anal. Chem*. **2016**, *88*, 11062-11069.

(26) Wang, W.; Kong, T.; Zhang, D.; Zhang, J. N.; Cheng, G. S. Label-Free MicroRNA Detection Based on Fluorescence Quenching of Gold Nanoparticles with a Competitive Hybridization. *Anal. Chem*. **2015**, *87*, 10822-10829.

(27) Su, J.; Wang, D. F.; Nörbel, L.; Shen, J. L.; Zhao, Z. H.; Dou, Y. Z.; Peng, T. H.; Shi, J. Y.; Mathur, S. J.; Fan, C. H.; Song, S. P. Multicolor Gold-Silver Nano-Mushrooms as Ready-to-Use SERS Probes for Ultrasenstive and Multiplex DNA/miRNA Detection. *Anal. Chem.* **2017**, *89*, 2531-2538.

(28) Alessandro, C.; Chiara, N.; Andrea, L.; Francesco, G.; Fabrizio, G.; Paola, R. Immobilization of Oligonucleotides on Metal-Dielectric Nanostructures for miRNA Detection. *Anal. Chem.* **2016**, *88*, 9554-9563.

(29) Masud, M. K.; Islam, M. N.; Haque, M.; Tanaka, H.; Gopalan, S.; Alici, V.; Nguyen, G. N. T.; Lam, K.; Hossain, M. S. A.; Muhammad, Y. Y.; Shiddiky, J. A. Gold-loaded Nanoporous Superparamagnetic Nanocubes for Catalytic Signal Amplification in Detecting miRNA. *Chem. Commun.* **2017**, *53*, 8231-8234.

(30) Liao, Y. H.; Huang, R.; Ma, Z. K.; Wu, Y. X.; Zhou, X. M.; Xing, D. Target-Triggered

Enzyme-Free Amplification Strategy for Sensitive Detection of MicroRNA in Tumor Cells and Tissues. *Anal. Chem.* **2014**, *86*, 4596-4604.

(31) Wang, Y. Z.; Ji, S. Y.; Xu, H. Y.; Zhao, W.; Xu, J. J. Chen, H. Y. Ultrasensitive microRNA Assay via Surface Plasmon Resonance Responses of Au@Ag Nanorods Etching. *Anal. Chem.* **2018**, *90*, 3570-3575.

(32) Brase, J. C.; Wuttig, D.; Kuner, R.; Sültmann, H. ; *Brase et al.* Serum microRNA as Non-invasive Biomarkers for Cancer. *Molecular Cancer.* **2010**, *9*, 306-315.

(33) Wang, Z. Y.; Han, J. X.; Cui, Y. Z.; Zhou, X. Y.; Fan, K. X. MiRNA-21 Inhibition Enhances RANTES and IP-10 Release in MCF-7 via PIAS3 and STAT3 Signalling and Causes Increased Lymphocyte Migration. *Biochem. Biophys. Res. Commun.* **2013**, *439*, 384-389.

for TOC Only

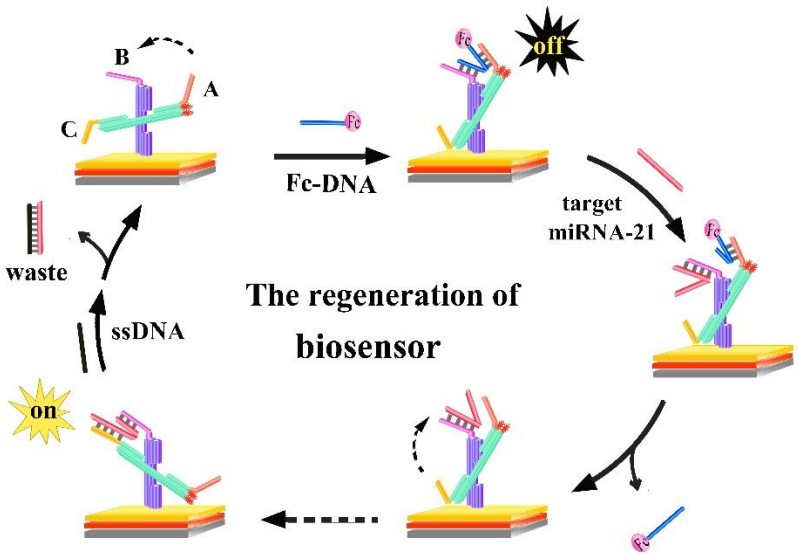
B
A
C
Fc
Fc-DNA
off
target
miRNA-21
Fc
Fc
The regeneration of
biosensor
waste
ssDNA
on